

Effect of Polypropylene Fiber Reinforced Concrete for Enhancing the Seismic Performance of Bridge Columns



T. Sasaki

National Research Institute for Earth Science and Disaster Prevention

R. Zafra

University of the Philippines Los Baños

K. Kawashima

Tokyo Institute of Technology

SUMMARY:

Bridges are vital components of transportation networks that require a high degree of protection to ensure their functionality during a strong earthquake. Damage after an earthquake may render the structure unusable which may interfere with disaster recovery operation as well as affect the economy of the community. To enhance the seismic performance and serviceability of bridges, focus has been on the development and implementation of innovative materials. In this study, polypropylene fiber reinforced cement composites (PFRC) is investigated as the materials which can mitigate the damage in plastic hinge region based on the loading experiments. In the loading experiments, longitudinal bars ruptured when the column displacement reaches 5.0% drift under cyclic loading, while longitudinal bars did not rupture until column displacement reaches 9.0% drift. Thus, it is found that PFRC columns has high ductility capacity if realistic loading condition is introduced in the loading program.

Keywords: seismic design, bridge column, polypropylene fiber reinforced cement composites, failure mechanism, ductility capacity

1. INTRODUCTION

Bridges are vital components of transportation networks that require a high degree of protection to ensure their functionality during a strong earthquake. Damage after an earthquake may render the structure unusable which may interfere with disaster recovery operation as well as affect the economy of the community. To enhance the seismic performance and serviceability of bridges, focus has been on the development and implementation of innovative materials. Since a bridge column sustains damage at the plastic hinge, the seismic performance of the column can be enhanced if the damage in plastic hinge region can be mitigated by using innovative materials, the seismic performance of the bridge columns can be enhanced.

Various fiber reinforced concrete/cement composites (FRC) with steel, polymeric, glass and carbon fibers have been developed. FRCs were first introduced in the 1960s by Romualdi (1963, 1964). The traditional FRCs developed in the early stage are characterized by a tensile strain softening response after reaching first cracking strength. However, recently, a new category of FRCs, referred to as high-performance fiber reinforced cement composites (HPFRCCs), were developed. They are characterized by a tensile strain-hardening response with multiple cracking. Larger strain capacity and ductility of HPFRCCs is appropriate for use in the plastic hinges. Use of HPFRCCs leads to improvement in ductility, toughness, fatigue resistance and deformation capacity (Matumoto and Mihashi, 2003).

Kawashima and Zafra et al. (2011) found that a column which used polypropylene fiber reinforced cement composites (PFRC) at the plastic hinge had higher ductility capacity than a column which used steel fiber reinforced concrete or normal strength reinforced concrete at the plastic hinge region. Kawashima and Zafra et al (2012) showed the effectiveness of PFRC column based on a shake table experiment using E-Defense for a 7.5 m tall full-size model. Kosa et al. (2007) conducted loading

experiments on RC columns in which the plastic hinge region was retrofitted by HPFRCCs with polyvinyl alcohol (PVA) fibers and found that the column using HPFRCC on the cover concrete can have the lateral confinement effect similar to a column in which the entire cross section was constructed by HPFRCCs.

In this study, two scaled model columns were loaded under bilateral cyclic loading and quasi-dynamic loading (seismic response loading) to study the progress of failure and the ductility capacity of the PFRC columns. Loading protocol dependence of the progress of failure and ductility capacity of PFRC columns is presented.

2. SCALED MODELS AND LOADING CONDITIONS

Two columns with the same size, reinforcement and materials were constructed for experiment under two loading conditions. The columns used PFRC at the plastic hinge region as shown in Fig 1. The geometrical scale was assumed to be 6/35 relative to the full-scale PFRC column (C1-6 column) excited by E-Defense (Kawashima and Zafra et al. 2012). C1-6 column was a 7.5 m tall and it had a 1.8 m by 1.8 m square section with round corner. It was designed for Level 2 design ground motions based on the 2002 JRA code assuming the moderate soil condition. In C1-6 column, PFRC was used in the plastic hinge region of the column within 2.7 m from the base and a part of the footing within 0.6 m from the surface. Eighty deformed longitudinal bars with a diameter of 35 mm were set in double in C1-6 column. Deformed tie bars with a diameter of 22 mm were set at every 150 mm and 300 mm interval for the outer and inner longitudinal bars, respectively. Two cross ties in the longitudinal and transverse directions each were set at every 150 mm.

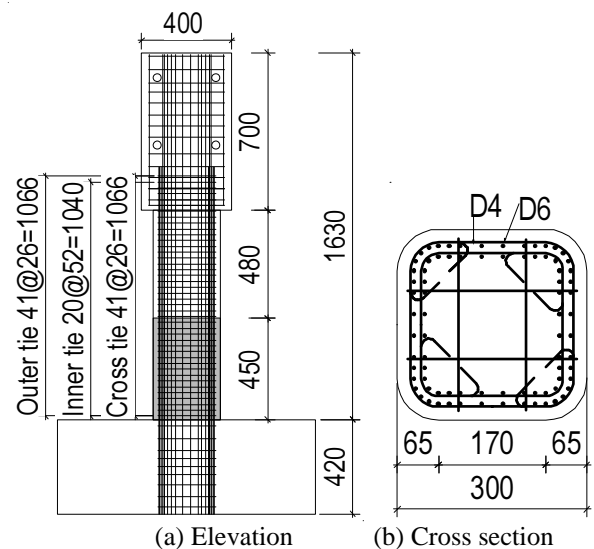


Figure 1. Experimental Specimen

C1-6 column was excited six times by Takatori ground acceleration which was recorded at JR-Takatori Station during the 1995 Kobe earthquake. It was one of the most destructive ground accelerations recorded during the Kobe earthquake. Since no radiational damping exists in C1-6 anchored to the table, direct excitation using the original ground motion results in excessive response than the normal condition that the footing and a part of the column are embedded in ground. Thus the intensity of original ground accelerations was reduced by 20% for taking account of the soil-structure interaction effect. This is called E-Takatori ground acceleration, and it was imposed to the table.

C1-6 column was excited in series. It was first excited twice by imposing 100 % E-Takatori ground acceleration under the design superstructure mass of 307 t. C1-6 column was then excited once under 100% E-Takatori ground acceleration after increasing the superstructure mass from 307 t to 372 t. C1-6 column was further excited three times under 125% E-Takatori ground acceleration.

Based on the geometrical scale of 6/35, two scaled models were designed such that they were 1.37 m tall from the base to the loading point (total height from the base to the top is 1.63 m) having a 0.3 m by 0.3 m square section with four 65 mm round corners. PFRC was used in the plastic hinge region within 450 mm from the base while the standard concrete was used in the rest including the footing. Note that a part of the footing was constructed by PFRC in C1-6 columns while regular concrete was used in the scaled model. As will be described later, this resulted in larger column failure at the base in the scaled models. The nominal strength of PFRC was 40 MPa and 3 % volume of polypropylene

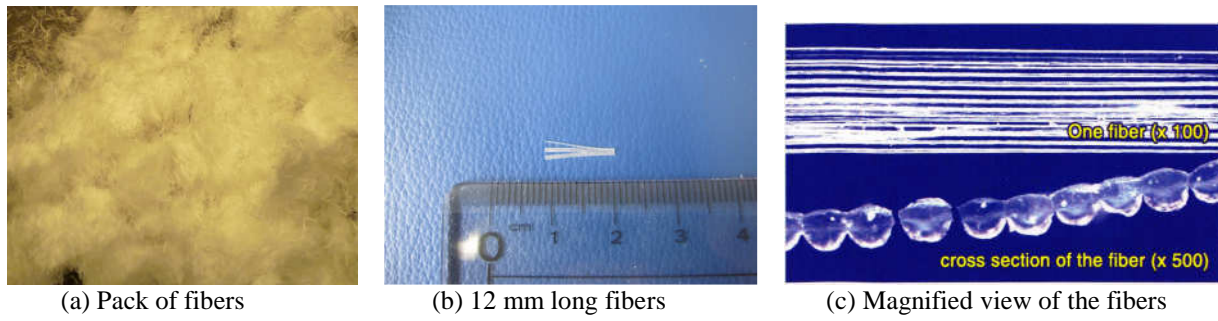


Photo 1. Polypropylene fibers used in the experiments

fibers were combined in the PFRC. The polypropylene fibers as shown in Photo 1 were used. They were 12 mm long fibrillated fibers with a diameter of $42.6 \mu\text{m}$, the tensile strength of 482 MPa and the Young's modulus of 5 GPa. Based on the coupon experiments, the compressive strength and tensile strength of PFRC were 40.1 MPa and 2.1 MPa, respectively, as shown in Fig. 2.

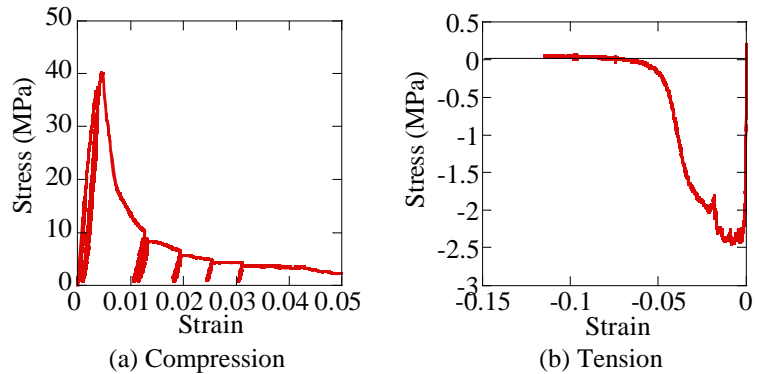


Figure 2. Stress vs. Strain Hysteresis of PFRC

Eighty deformed longitudinal bars with a diameter of 6 mm and the nominal yield strength of 345 MPa were set in double in the models. Deformed bars with a diameter of 4 mm and the nominal yield strength of 295 MPa were set at every 26 mm for outer ties and at every 52 mm for inner ties. Four cross ties were provided at every 26 mm in the column within 450mm from the base while two cross ties were provided every 26mm in the column higher than 450 mm from the base. Volumetric tie bar ratio in the model columns was 1.72 % which was the same with the volumetric tie bar ratio of C1-6 column. Based on the tensile tests of the deformed bars, yield strength of the longitudinal bars and ties were 386 MPa and 396, respectively.

Photo 2 shows the experimental setup. Two loading protocols were used. The first model was subjected to a bilateral cyclic loading assuming a circular orbit under a constant vertical compression force of 88 kN. The model was first loaded in the East (E) direction until the displacement reached 0.5 % drift at the loading point. From this point, the model was loaded three times along the circular orbit. Finally, the pier was unloaded to the rest position from the E direction. This set of loadings was repeated until failure of the model with an increment of 0.5 % drift, where drift is defined as a ratio between a column displacement at the loading point divided by the distance between the base and the loading point (1.37 m)

On the other hand, the other scaled column model was loaded such that the seismic response of C1-6 column could be reproduced in the scaled model considering the similarity law. Because the lateral response displacements of C1-6 column in the longitudinal and transverse directions were measured at its top, they were imposed to the scaled model at the loading point, under the displacement control, in the respective directions by reducing the amplitude of measured response displacement by $6/35$. In a similar way, because the vertical force applied to the C1-6 column at the base was measured, it was imposed to the scaled model at the top, under the

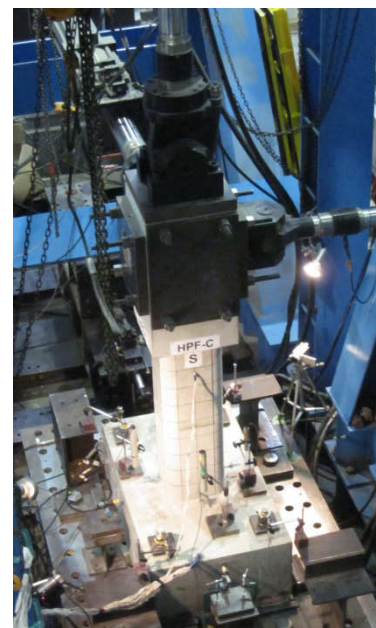


Photo 2. Experimental Setup

force control, by reducing the force amplitude by $(6/35)^2$. Such a loading is called herein "seismic response loading."

Note that because there are geometrical interactions between three components of loading displacements, they were modified in the process of imposing the lateral displacements and the vertical force (Nagata et al. 2004). Note also that loading rate was 1/10 slower in the seismic response loading, however it is known that the effect of loading rate on the seismic performance of bridge columns is less significant as long as the loading rate is less than 1 m/s (Kawashima et al. 1987). The scaled model column was loaded six times corresponding to the shake table experiments of the C1-6 column. The scaled model column was further loaded under 125 %, 150 % and 180 % increased lateral displacements which occurred during the 6th excitation.

3. PROGRESS OF FAILURE OF PFRC COLUMNS

3.1. Progress of failure of a PFRC column under cyclic loading

Photo 3 shows the progress of damage at the plastic hinge region under the cyclic loading. During 1.5 % drift loading, flexure cracks opened as wide as 0.08 mm. A crack opened between the footing and the column during the 1.5 % drift loading. During the 2.0 % and 2.5 % drift loadings, the crack width increased to 0.15 mm and 0.2 mm, respectively. During the 2.5 % drift loading, a major vertical crack as wide as 0.45 mm opened at a corner at the base. The concrete at a part of the surface of footing within 50 mm from the column crushed during the 2.5 % drift loading. During the 4.0 % and 4.5 % drift loading, a lateral actuator touched to the steel frame resulting in some increase of the measured restoring force as will be described later. During the 5.0 % drift loading, at least five longitudinal bars ruptured. During the 5.5 % drift loading, longitudinal bars further ruptured. Since the restoring force significantly deteriorated, the cyclic loading was completed.

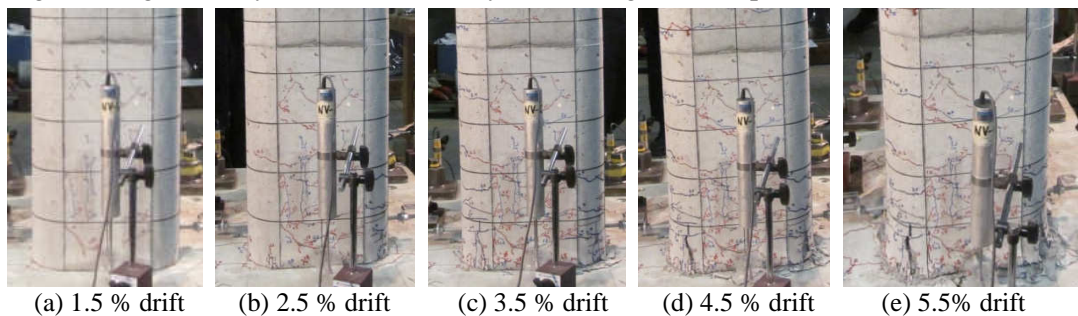


Photo 3. Progress of Damage in the Plastic Hinge Region under Cyclic Loading



Photo 4. Damage in the Plastic Hinge Region after Cyclic Loading Experiment

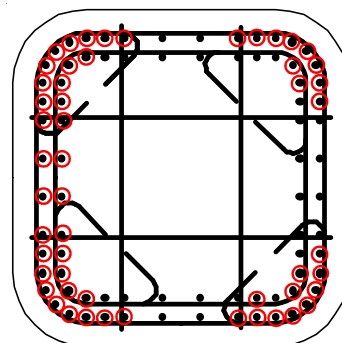


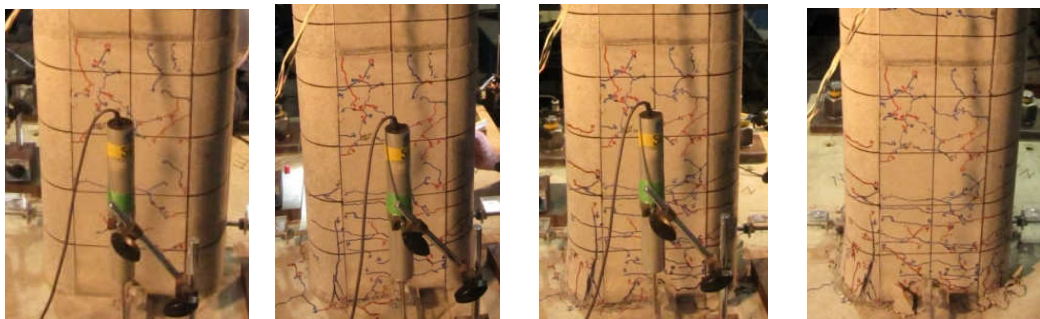
Figure 3. Raptured Longitudinal Bars in Cyclic Loading Experiment

Photo 4 shows damage of the column at the plastic hinge region after the cyclic loading was completed and covering concrete was removed. At the column base, 37 outer longitudinal bars and 17 inner longitudinal bars ruptured as shown in Fig. 3. The concrete at the footing surface crushed as deep as 30 mm and this lead to local buckling of several longitudinal bars. For mitigating such a

failure of the footing surface and local buckling of longitudinal bars, it may be effective to use PFRC in the upper part of the footing such as C1-6 column.

3.2. Progress of failure of a PFRC column under seismic response loading

Photo 5 shows the damage of the column at the plastic hinge region after the 3rd, 5th, 8th and 9th seismic response loading was completed. During the 1st, 2nd and 3rd excitations with the peak lateral drift of 1.1 %, 1.2 % and 1.9 %, respectively, only flexural cracks as large as 0.06-0.15 mm occurred. During the 4th excitation, the peak lateral drift of the column was 3.7 % drift, and a major vertical crack occurred at the SW corner and it extended during the 5th excitation (the peak lateral drift was 5.1 % drift) as shown in Photo 5(b). During the 6th and 7th excitations (the peak lateral drift was 6.0 % and 7.5 % respectively), the vertical cracks further extended however PFRC did not suffer extensive damage without deterioration of the flexural restoring force. During the 8th excitation, the peak column displacement reached 9.0% drift, and at least four longitudinal bars ruptured. Since longitudinal bars started to rupture during 5.0 % drift loading under the cyclic loading, the 9.0 % drift at which longitudinal bars started to rupture under the seismic response loading was 1.8 times larger. After the 9th excitation, the flexural restoring force deteriorated.



(a) After 3rd excitation (b) After 5th excitation (c) After 8th excitation (d) After 9th excitation

Photo 5. Progress of Damage in the Plastic Hinge Region under Seismic Response Loading



Photo 6. Damage in the Plastic Hinge Region after Seismic Response Loading Experiment

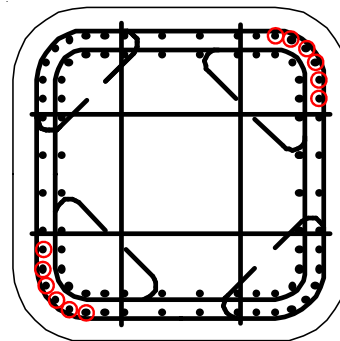


Figure 4. Ruptured Longitudinal Bars after Seismic Response Loading Experiment

Photo 6 shows the damage of the column after the 9th seismic response loading experiment and Fig. 4 shows the locations of ruptured longitudinal bars. As shown in Fig. 4, 12 outer longitudinal bars ruptured, however, no inner longitudinal bar ruptured. Consequently, the number of ruptured bars under the seismic response control was nearly 1/4 of the number of ruptured bars under cyclic loading. Therefore, the effect of loading protocols on the damage of the model columns is significant. Similar to the damage under the cyclic loading, the concrete at the footing surface crushed as deep as 30 mm and local buckling of longitudinal bars were developed there under the seismic response loading too.

4. STRAINS OF REBARS

Fig. 5 shows strains of a longitudinal bar at the base and 52 mm and 104 mm from the base at SW

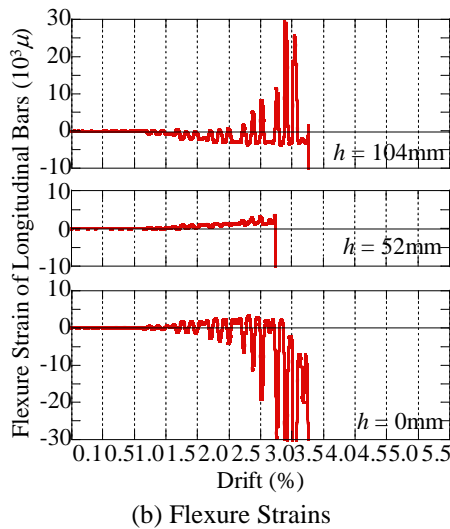
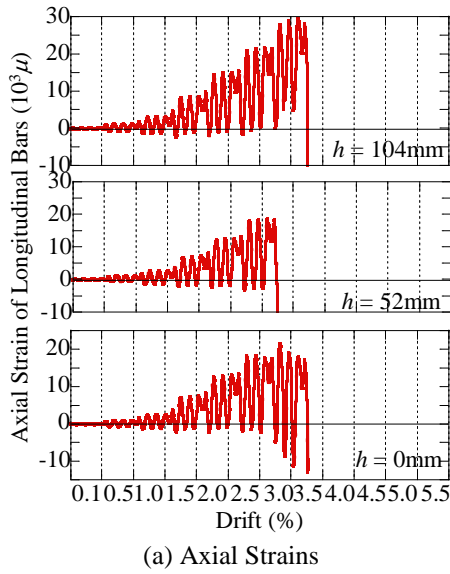


Figure 5. Strains of a Longitudinal Bar at SW Corner under Cyclic Loading

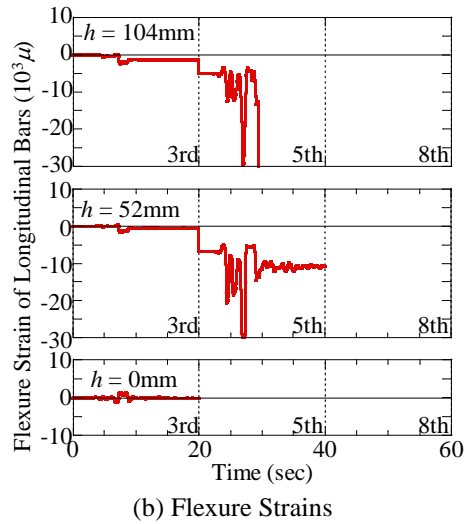
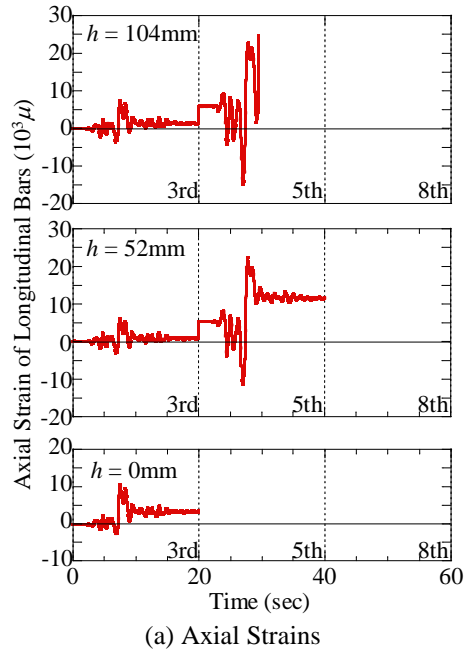


Figure 6. Strains of Longitudinal Bars at SW Corner under Seismic Response Loading

corner in the column subjected to the cyclic loading. Both axial and flexural strains are shown here. Axial strains of the longitudinal bar gradually increases from 1.0% drift. On the other hand, the flexural strains started to sharply increase at 2.5% drift which shows that local buckling of the longitudinal bar occurred.

Fig. 6 shows strains of a longitudinal bar at the same locations in the column subjected to the seismic response loading. Axial strains started to increase at the 3rd excitation, and they reached over 20,000 μ at the 5th excitation. On the other hand, the flexural strain started to increase at the 4th excitation, and they extensively increased at the 5th excitation indicating that local buckling of the longitudinal bar became predominant.

Figs. 7 and 8 show axial strains of a tie, at three locations (west side, center and east side) 67 mm from the base located in EW direction under the cyclic loading and the seismic response loading, respectively. It is noted that the strains are similar between the three locations.

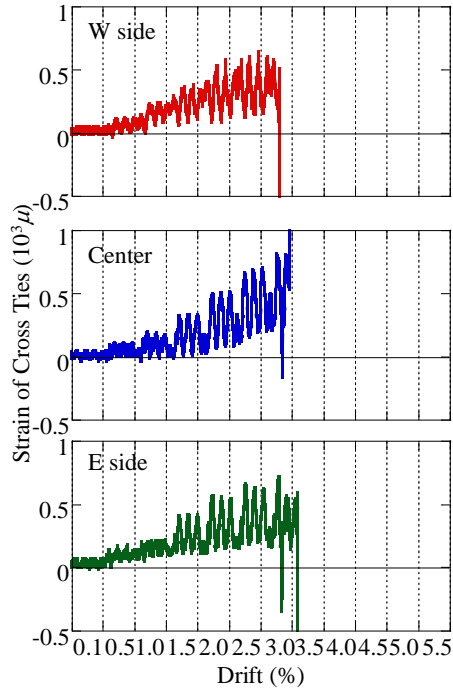


Figure 7. Strains of Cross Tie at 67mm from the base in EW direction under Cyclic Loading

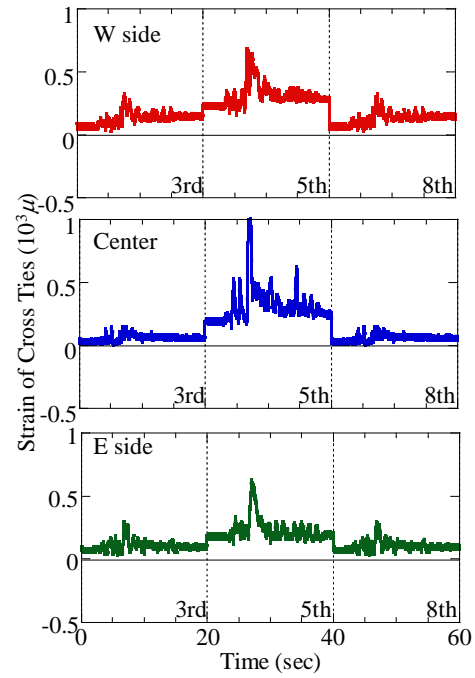


Figure 8. Strains of Cross Ties at 67mm from the base in EW Direction under Seismic Response Loading

5. MOMENT CAPACITY

Figs. 9 and 10 show hysteresis of the flexural moment at the column base vs. the lateral displacement at the loading point under the cyclic loading and the seismic response loading, respectively. The hystereses in the NS and EW direction are shown here. Since the moment capacity was similar between the EW and NS directions, the flexural moment in the EW is shown below. The flexural moment reached the maximum value of 122 kNm when the drift reached 2.0 %. At 5.5 % drift, the moment deteriorated to 87 kNm which was 71 % of the maximum flexural moment. On the other hand, the maximum flexural moment was 133 kNm at the 5th excitation (4.6 % drift). Even during the 8th excitation (8.1 % drift), the maximum flexural moment was 126 kNm which is 95 % of the flexural moment during the 5th excitation.

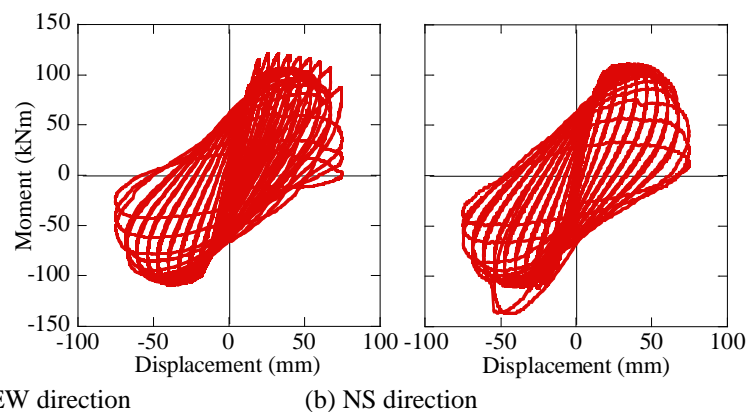


Figure 9. Moment at the Base vs. Lateral Displacement at the Loading Point Hysteresis under Cyclic Loading

Fig. 11 compares the peak flexural moment at the column base vs. the peak drift at the loading point curves. It is noted that the moment capacity of the model column was larger under the seismic response control than the cyclic loading. Rupture of longitudinal bars at the earlier loading stage deteriorated the column flexural capacity. It is also noted that under the cyclic loading, the flexural moment started to sharply deteriorate at 5.5 % drift while the flexural moment did not deteriorate even

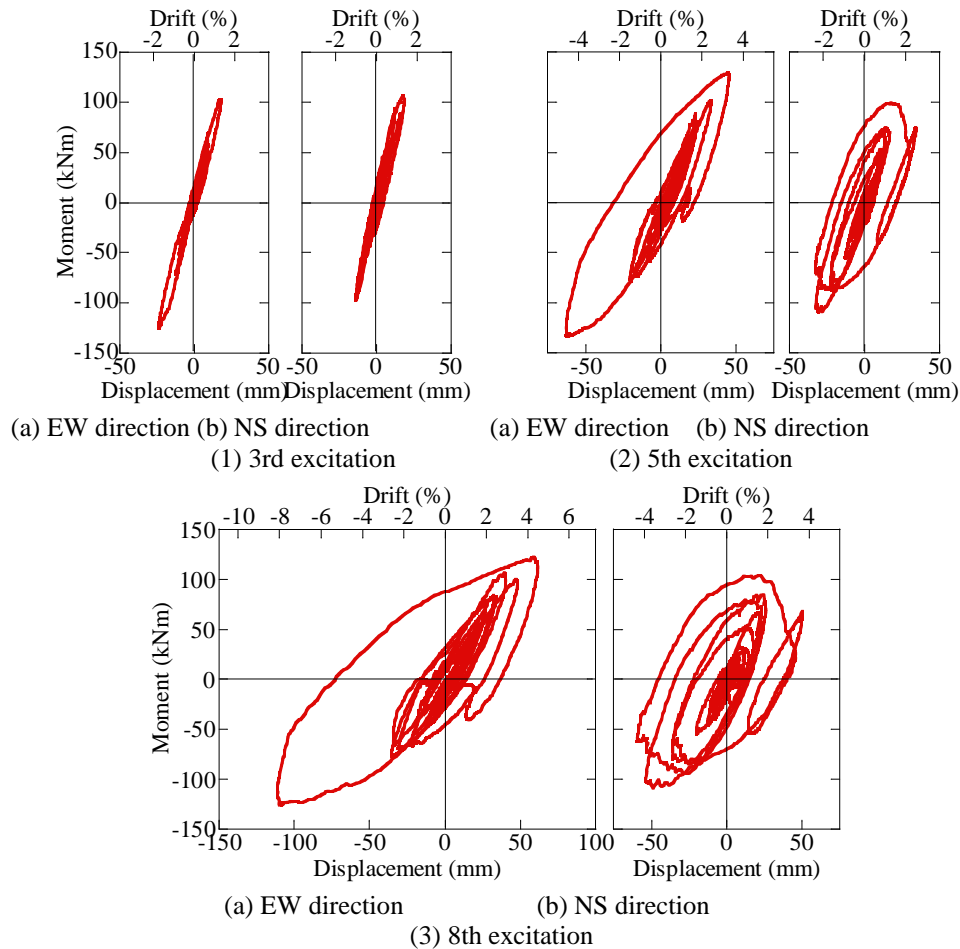


Figure 10. Moment at the Base vs. Lateral Displacement at the Loading Point Hysteresis under Seismic Response Loading

at 8.1 % drift under the seismic response loading. The rupture of longitudinal bars at the early stage also decreased the column ductility factor. Thus the loading protocol dependence of the column flexural capacity and ductility capacity should be properly evaluated for column capacity. The PFRC model column showed significantly high ductile behaviour under the seismic response loading.

6. CONCLUSIONS

Polypropylene fiber reinforced cement composites (PFRC) was implemented to two 6/35 scaled bridge columns, and the fundamental failure mechanism was investigated based on a bilateral cyclic loading assuming circular orbit and the seismic response loading which aimed of simulating the seismic response of full-size C1-6 column subjected to a ground acceleration recorded at JR Takatori Station during the 1995 Kobe earthquake. An emphasis was placed on the loading condition dependence of the progress of failure. Based on the study presented herein, the following conclusions may be deduced;

1) The moment capacity of the model column was larger under the seismic response control than the cyclic loading. Rupture of longitudinal bars at the earlier loading stage deteriorates the column flexural capacity.

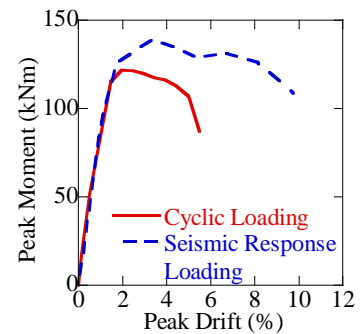


Figure 11. Peak Moment at the Column Base vs. Peak Drift at the Loading Point Hysteresis in the longitudinal direction

- 2) Under the cyclic loading, the flexural moment started to sharply deteriorate at 5.5 % drift while the flexural moment did not deteriorate even at 8.1 % drift under the seismic response loading. The rupture of longitudinal bars at the early stage also decreased the column ductility factor.
- 3) Loading protocol dependence of the column flexural capacity and ductility capacity should be properly evaluated for column capacity.
- 4) The PFRC model column showed significantly high ductile behaviour under the seismic response loading.

ACKNOWLEDGEMENT

This study was funded by Japan Institute of Construction Engineering (Grant No. 09002). Polypropylene fiber reinforced cement composites were provided by Dr. Hirata, T., Obayashi Corporation, and the authors appreciate invaluable advice and kind support for design of the specimens. Kind cooperation by Dr. Matsuzaki, H., Messrs. Kumagai, Y., Wang, J., Ohta, K., Ichikawa, S., Hirai, Y., Zhang, W. and Oya, T. for the experiment is acknowledged.

REFERENCES

- Kawashima, K., Hasegawa, K., Koyama, T. and Yoshida, T. (1987). Effects of loading velocity on dynamic behavior of reinforced concrete bridge piers, *Civil Engineering Journal*, **29-11**, pp. 3-8.
- Kawashima, K., Zafra, R., Sasaki, T., Kajiwar, K., and Nakayama, M. (2011). Effect of polypropylene fiber reinforced cement composite and steel fiber reinforced concrete for enhancing the seismic performance of bridge columns, *Journal of Earthquake Engineering*, **15**, pp. 1194-1211.
- Kawashima, K., Zafra, R., Sasaki, T., Kajiwar, K., Nakayama, M. Unjoh, S., Sakai, J., Takahashi, Y., Yabe, M. (2012). Seismic performance of a full-scale polypropylene fiber reinforced cement composite bridge column based on E-Defense shake table experiments, *Journal of Earthquake Engineering*, in print.
- Kesner, K., Billington, S. L. and Douglas, K. S. (2003). Cyclic response of highly ductile fiber-reinforced cement based composites, *ACI Materials Journal*, **100(5)**, pp. 381-390.
- Kosa, K., Wakita, K., Goda, H. and Ogawa, A. (2007). Seismic strengthening of piers with partial use of high ductility cement, in *Advances in Construction Materials*, ed. C. U. Grosse, Springer, pp. 269-277, Berlin Heidelberg.
- Matsumoto, T. and Mihashi, H. (2003). DFRCC terminology and application concepts, *Journal of Advanced Concrete Technology*, **JCI 1(3)**, pp. 335-340.
- Nagata, S., Kawashima, K., and Watanabe, G. (2004). Effect of P- Δ action of actuators in a hybrid loading test, *Proc. 13th World Conference on Earthquake Engineering*, **Paper No. 881**, Vancouver, Canada.
- Romualdi, J.P. and Batson, G.B. (1963). Mechanics of crack arrest in concrete, *Proc. ASCE Journal of Engineering Mechanics Division*, **89, EM3**, pp. 147-168.
- Romualdi, J.P. and Mandel, J.A. (1964). Tensile strength of concrete affected by uniformly distributed and closely spaced short lengths of wire reinforcement, *ACI Journal Proceedings*, **61**, pp. 657-670.